Posttranscriptional modulation of KCNQ2 gene expression by the miR-106b microRNA family

Kwon-Woo Kim[a,1], Keetae Kim[b,1,2], Hee-Jin Kim[c], Byeol-I Kim[a], Myungin Baek[a], and Byung-Chang Suh[a,2]

[a]Department of Brain and Cognitive Sciences, Daegu Gyeongbuk Institute of Science and Technology, Daegu 42988, Republic of Korea; [b]Department of New Biology, Daegu Gyeongbuk Institute of Science and Technology, Daegu 42988, Republic of Korea; and [c]Center for Plant Aging Research, Institute for Basic Science, Daegu 42988, Republic of Korea

Edited by Bruce P. Bean, Harvard Medical School, Boston, MA, and approved October 12, 2021 (received for review June 2, 2021)

MicroRNAs (miRNAs) have recently emerged as important regulators of ion channel expression. We show here that select miR-106b family members repress the expression of the KCNQ2 K^+ channel protein by binding to the 3′-untranslated region of KCNQ2 messenger RNA. During the first few weeks after birth, the expression of miR-106b family members rapidly decreases, whereas KCNQ2 protein level inversely increases. Overexpression of miR-106b mimics resulted in a reduction in KCNQ2 protein levels. Conversely, KCNQ2 levels were up-regulated in neurons transfected with antisense miRNA inhibitors. By constructing more specific and stable forms of miR-106b controlling systems, we further confirmed that overexpression of precursor-miR-106b-5p led to a decrease in KCNQ current density and an increase in firing frequency of hippocampal neurons, while tough decoy miR-106b-5p dramatically increased current density and decreased neuronal excitability. These results unmask a regulatory mechanism of KCNQ2 channel expression in early postnatal development and hint at a role for miR-106b up-regulation in the pathophysiology of epilepsy.

KCNQ2/3 K+ channel | miRNA | miR-106b family | developmental regulation | KCNQ2 protein

MicroRNAs (miRNAs) are single-stranded small noncoding RNA molecules with ∼22 nucleotides, which bind the 3′-untranslated region (3′-UTR) or coding region (CDS) of their target messenger RNAs (mRNAs) and regulate protein synthesis by destabilizing the mRNA or arresting the translation process (1–3). About 50% of mammalian miRNAs are expressed in the brain (4, 5) and play important roles in neurogenesis and neuronal development (6, 7). Recent studies have identified miRNAs as potential novel and noninvasive diagnostic biomarkers for epilepsy syndrome (8, 9). The functional role of miRNAs in epilepsy is mostly related to regulation of ion channel expression in central and peripheral nervous systems (10, 11). Several voltage-gated ion channels, such as Kv1.1, Kv4.2, $Na_V1.1$, GluA2, and GluN2B are known to be regulated at the translational stage by miRNAs. Recent genome-wide miRNA expression profiling studies using the serum of epilepsy patients suggested that miR-106b expression is elevated in pediatric patients with epileptic syndromes (12, 13). Subsequent evaluation of the association between biomarkers and clinical parameters of epilepsy established that among the selected miRNAs whose expression levels were altered in epilepsy patients, including up-regulated let-7d, miR-106b, miR-130a, miR-146a, and down-regulated miR-15a and miR-194, miR-106b possessed the greatest diagnostic capability for epilepsy (14, 15). However, target molecules for miR-106b that might illuminate its mechanistic role in epileptogenesis were not clearly defined.

KCNQ2/KCNQ3 (KCNQ2/3) heterotetrameric voltage-dependent channels are broadly expressed in the brain and are known to conduct the muscarine-sensitive M-current, which contributes to a slowly activating and deactivating potassium current (16–19). The two KCNQ2 and KCNQ3 subunits are colocalized at the soma, dendrites, and axon-initial segments (AIS) of pyramidal neurons in central nervous systems (20, 21). As its threshold for channel activation is more negative than that of other potassium channels, the KCNQ2/3 channel plays a crucial role in regulating resting membrane potential and cell excitability. Thus, inhibition of this channel usually results in an increase in action potential (AP) generation with reduced spike-frequency adaptation (22–25). Previous studies have reported that a single mutation in the KCNQ2/3 channel reduces the current by ∼25% compared with wild-type (WT) channels, leading to an abnormal increase in neuronal excitability (26). Similarly, overexpression of a KCNQ2 subunit with a dominant-negative mutation generated seizures and hyperexcitability in hippocampal neurons (18, 25, 27). Interestingly, most KCNQ2 knockout mice die within 3 wk, whereas genetic deletion of KCNQ3 gene does not cause any changes in excitability and permits survival into adulthood (28–30). Therefore, the KCNQ2/3 channel has been considered as a therapeutic target in many other brain disorders as well as in general epilepsy (31–33).

Since the expression of KCNQ2 and KCNQ3 mRNAs increases rapidly in the brain during the first few weeks of life, the KCNQ2/3 channel complex plays a crucial role in determining the excitability of developing neurons during this period (34, 35). Western blot analysis of various regions of the brain, such as the hippocampus, temporal cortex, cerebellar cortex,

Significance

Up-regulation of the M-type KCNQ2/KCNQ3 channels from late fetal life to early infancy is important for normal development and functional maturation of nervous systems in the brain. However, detailed mechanisms for the early regulation of KCNQ2/3 expression remain unclear. Here, we report that select miR-106b microRNA (miRNA) family members modulate the KCNQ2 subunit expression by binding to the 3′-untranslated region of KCNQ2 messenger RNA. Moreover, KCNQ2 expression and miR-106b family members are inversely regulated in early stages of the mouse hippocampus, revealing the mechanisms underlying the sustained increase of KCNQ channel activity during postnatal development. Our work will provide insight into why miR-106b miRNA is the key biomarker for epileptic syndromes.

Author contributions: K.K. and B.-C.S. designed research; K.-W.K., K.K., H.-J.K., B.-I.K., and M.B. performed research; B.-I.K. contributed new reagents/analytic tools; K.-W.K., K.K., H.-J.K., and M.B. analyzed data; K.-W.K., K.K., M.B., and B.-C.S. wrote the paper; and B.-C.S. supervised the project.

The authors declare no competing interest.

This article is a PNAS Direct Submission.

Published under the PNAS license.

[1]K.-W.K. and K.K. contributed equally to this work.

[2]To whom correspondence may be addressed. Email: keetae11@gmail.com or bcSuh@DGIST.ac.kr.

This article contains supporting information online at http://www.pnas.org/lookup/suppl/doi:10.1073/pnas.2110200118/-/DCSupplemental.

Published November 16, 2021.

and medulla oblongata, showed that the expression level of KCNQ2 and KCNQ3 proteins from late fetal life to early infancy is up-regulated, and this increase of KCNQ expression is essential for normal development and functional maturation of neurons (36, 37). However, detailed mechanisms for the early developmental regulation of KCNQ2/3 expression remain unclear. The ontogenies of KCNQ2 and KCNQ3 mRNAs in vivo exhibited regional and developmental differences in brain tissues such that levels of KCNQ2 mRNA transcript are relatively higher in embryonic and newborn stages, while the KCNQ3 mRNA level is low in those stages but steadily increases during early postnatal development (38, 39). Based on approaches using bioinformatics, RNA sequencing (RNA-seq), and cell biological analyses, we found here that select miR-106b family members, including miR-106, miR-17, and miR-20a, down-regulate KCNQ2 protein expression by binding to the 3′-UTR of KCNQ2 mRNA, leading to increased neuronal excitability in early developing rodent hippocampal and cortical neurons. On the other hand, knockdown of these miRNAs leads to an increase in KCNQ2 protein expression and a decrease in neuronal excitability. Our results provide insight into the regulatory mechanisms of KCNQ2 gene expression during early development, establishing functional roles of miR-106b family miRNAs in the stage-specific occurrence of epileptic syndromes.

Results

miR-106b Family miRNAs Repress KCNQ2 Protein Expression by Binding to the Target Site on the 3′-UTR of KCNQ2 mRNA. As miRNAs continue to emerge as important regulators of their target channel proteins (11), we searched for conserved miRNA candidates on the 3′-UTR of the KCNQ2 gene using three different miRNA prediction databases: Targetscan (http://www.targetscan.org/vert_80/), Miranda (https://cbio.mskcc.org/miRNA2003/miranda.html), and miRDB (http://mirdb.org/). The consensus for all three databases indicated that five miRNAs, including miR-17, miR-20a, miR-93, miR-106a, and miR-106b, could serve as highly conserved regulators of KCNQ2 expression (Fig. 1*A*). We considered all five miRNAs as members of the miR-106b family based on the high similarity of their nucleotide sequences, including the conserved seed motif (Fig. 1*B*) (40). Indeed, our small RNA-seq analysis indicated that miR-17, miR-20a, miR-93, and miR-106b were highly expressed at P0 in mouse hippocampal tissues (Fig. 1*C*). Since there was no detectable amount of miR-106a at P0 in the hippocampus, we focused on the remaining four miRNAs as candidates for KCNQ2 modulators. Detailed sequence analysis predicted that they bind to the same sequence (target site) "GCACUUU" starting 188 nucleotides downstream from the end of the mouse KCNQ2 coding sequence (Fig. 1*D*). This putative seven-nucleotide miRNA-binding target site was also observed in the KCNQ2 3′-UTR of a subset of vertebrate species including rats, humans, pigs, bats, salmon, cows, dogs, cats, and chickens (*SI Appendix*, Fig. S1). Interestingly, the target site was also found in the CDS of several species, including humans, whales, and red foxes, but the nucleotide sequences surrounding it were quite different from those of the 3′-UTR (Fig. 1*D* and *SI Appendix*, Fig. S1). Broughton et al. (41) reported that additional base pairing between the 3′-region of miRNA and its target mRNA is a critical determinant of the specificity of miRNA–mRNA interactions.

We then tested whether each member of the miR-106b family has the potential to repress KCNQ2 expression in living cells. For this assay, we generated a reporter construct (pLuc-KCNQ2 WT 3′-UTR) in which the WT 3′-UTR of the KCNQ2 gene (miRNA-bound region) was fused to the luciferase gene (LUC). Cotransfection of pLuc-KCNQ2 WT 3′-UTR with either miR-17, miR-20a, or miR-106b mimics reduced luciferase activity by 30% ($P < 0.05$), 32% ($P < 0.05$), and 54% ($P < 0.01$), respectively, compared with each scrambled control (Fig. 2*A*). However, cotransfection with a miR-93 mimic, which exhibits less base pairing around the seed motif, did not cause any significant changes in luciferase activity (Fig. 2*A* and *SI Appendix*, Fig. S2), suggesting that the nucleotide alignment near the seed is also important in the interaction of miRNAs with target KCNQ2 mRNA. To examine the effect of mutation of miR-106b family binding sites on KCNQ2 repression, we generated a mutant reporter construct (pLuc-KCNQ2 Mut 3′-UTR) in which four nucleotide mismatch mutations were introduced on the binding sequence in the KCNQ2 3′-UTR (Fig. 2*A* and *SI Appendix*, Fig. S2). Cotransfection of pLuc-KCNQ2 Mut 3′-UTR with either miR-17, miR-20a, or miR-106b mimics did not induce any significant changes in luciferase activity compared to scrambled controls (Fig. 2*A*), indicating that the interaction of miR-17, miR-20a, and miR-106b miRNAs with their binding sequences within the KCNQ2 3′-UTRs are site specific. We did not observe any additive effects between the two miR-106b and miR-17 mimics or the two inhibitors in a quantitative luciferase assay in SV40 large T-antigen-transformed human embryonic kidney 293 (HEK293T) cells.

We then examined whether miR-106b family miRNAs play a role in regulating KCNQ2 protein synthesis in hippocampal neurons. Primary hippocampal neurons at 2 d in vitro (DIV2) were transfected with plasmids expressing miR-106b mimic or scramble miRNA and harvested at DIV7 for KCNQ2 protein assessment. As shown in Fig. 2*B*, transfection with miR-106b mimic miRNA significantly repressed KCNQ2 expression by ∼40% ($P < 0.05$) compared to that of cells with transfected with scramble control sequences. Conversely, transfection of an miR-106b antisense inhibitor led to a greater than 70% increase ($P < 0.01$) in KCNQ2 protein level (Fig. 2*B*). Expression of miR-17 or miR-20a mimics also repressed KCNQ2 expression by ∼27 and ∼23% ($P < 0.05$), respectively (Fig. 2*C*). However, miR-93 mimic did not cause any significant KCNQ2 repression in neurons. Together, our results demonstrate that although miR-106b, miR-17, and miR-20a have similar nucleotide sequences (Fig. 1*B*), miR-106b is more effective in regulating KCNQ2 protein expression. This is most likely due to its higher potency in paring with the nucleotides surrounding the seed sequence.

KCNQ2 Expression and miR-106b Family Members Are Inversely Regulated during Early Developmental Stages in the Mouse Hippocampus. Since KCNQ2 channel proteins are up-regulated during early developmental stages (34, 36), we measured the time-dependent expression of miR-106b family members. Our small RNA-seq data show that cellular levels of miR-106b family members, except miR-106a, which is almost absent at P0, gradually declined up to P60 (Fig. 3*A* and *SI Appendix*, Table S1). Since miR-106b effectively down-regulated KCNQ2 protein expression within 1 wk in transfection assays, we measured changes in miR-106b levels using real-time qPCR analysis of early developmental mouse hippocampal tissues isolated at time points ranging from P0 to P28. As shown in Fig. 3*B*, the level of miR-106b was highest at P0 and dramatically decreased up to 20% of the initial level at P21. The expression levels of miR-17-5p and miR-20a-5p were similarly down-regulated during the same period (Fig. 3*B*).

The developmental regulation of KCNQ2 expression was evaluated by Western blot analysis of mouse hippocampal tissues obtained at five different stages: P0, P7, P14, P21, and P28 (Fig. 3 *C*, *Top*). Expression of KCNQ2 protein was detectable but very low at P0 and was dramatically up-regulated by a factor of 3.7 at P21 (Fig. 3 *C*, *Bottom*). In the same hippocampal tissues, KCNQ2 mRNA was minorly changed at P7 (a factor of 1.5 ± 0.4), and the level remained relatively stable until P28

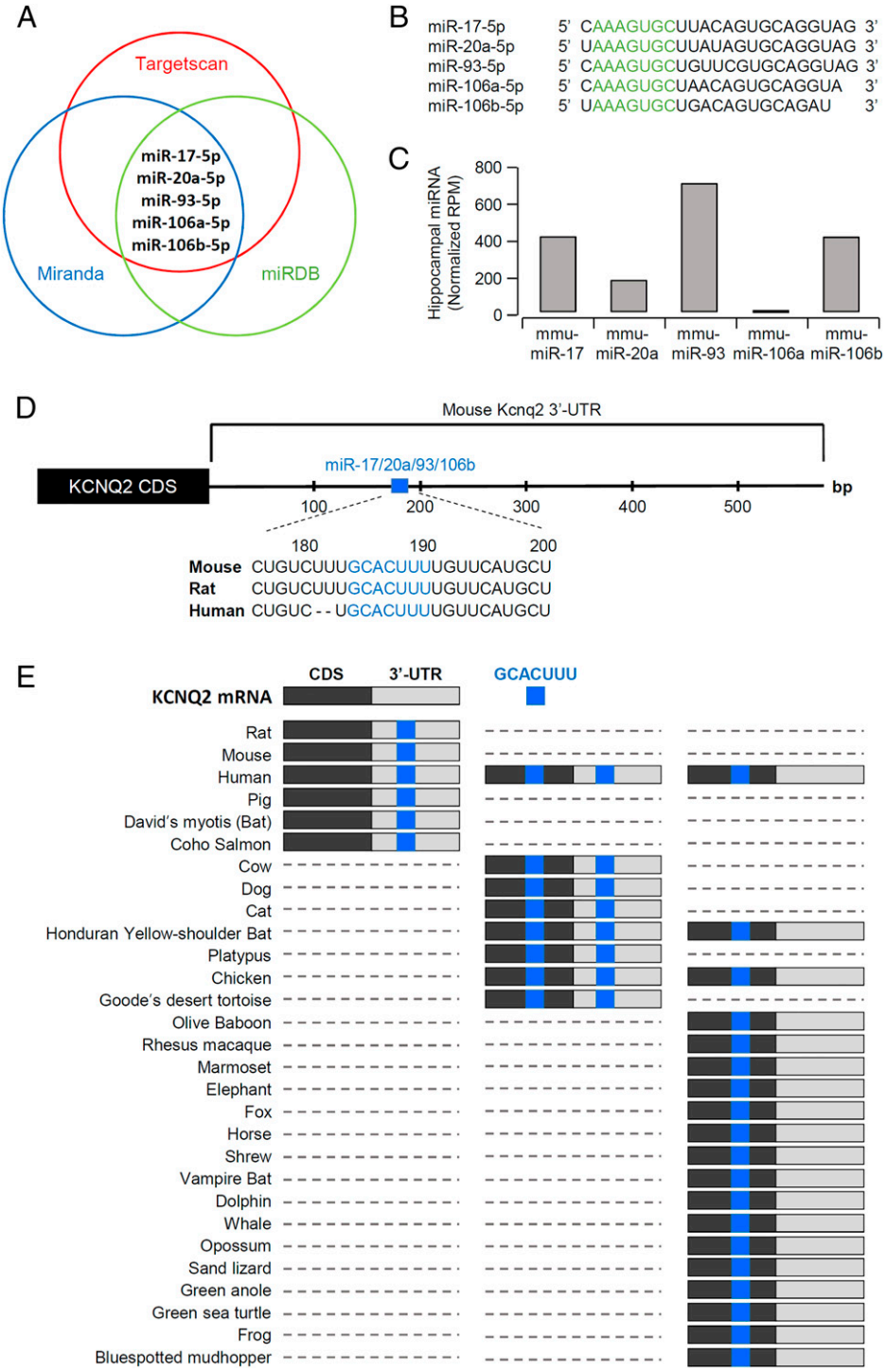

Fig. 1. miR-106 family miRNAs target a conserved region in the 3'-UTR of KCNQ2 mRNA. (*A*) Three different miRNA target prediction programs (Targetscan, Miranda, and miRDB) predicted that KCNQ2 mRNA has a conserved binding site for miR-106b family miRNAs including miR-17-5p, miR-201-5p, miR-93-5p, miR-106a-5p, and miR-106b-5p, indicating a possible posttranscriptional gene-expression regulatory pathway. (*B*) Nucleotide sequence of miR-106b family members. Seed sequence is shown in green. (*C*) Normalized read count per million (RPM) for miR-17-5p, miR-20a-5p, miR-93-5p, and miR-106b-5p expression at P0 stage in mice hippocampus. Note that miR-106a-5p was not detectable in P0 hippocampal tissues. (*D*) KCNQ2 3'-UTR has a target binding sequence (GCACUUU) for miR-106b family miRNAs. The common target site is highly conserved in the 3'-UTR of KCNQ2 mRNA in many mammalian species including mice, rats, and humans. (*E*) Conservation of miR-106b family–interacting target site in vertebrates. Shown is the summary of the National Center for Biotechnology Information Basic Local Alignment Search Tool (BLAST) result using the miR-106b–responsive conserved target sequence (GCACUUU). The presence of target site (blue) is indicated in CDS (dark gray) and 3'-UTR (gray). The position of the target site in each region is arbitrarily indicated, and the nucleotide numbers of target sequences are not included.

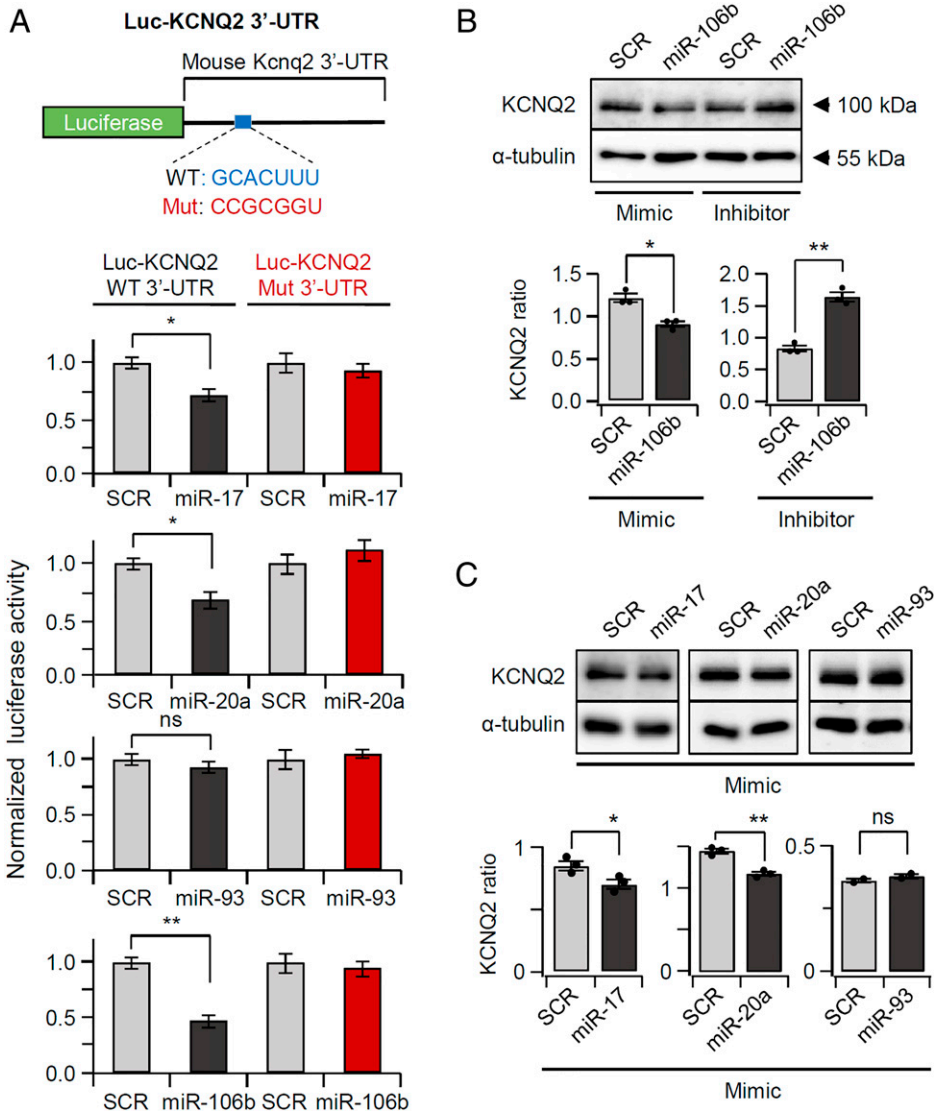

Fig. 2. KCNQ2 protein expression is modulated by select miR-106 family miRNAs. (*A*) Normalized luciferase activity in HEK293T cells transfected with recombinant firefly luciferase-mouse KCNQ2 3'-UTR (Luc-KCNQ2 WT 3'-UTR) reporters and miRNA-expressing plasmids or scrambles. The target sequence GCACUUU was changed to CCGCGGU in mutant 3'-UTR (Luc-KCNQ2 Mut 3'-UTR) reporters. Data are mean ± SEM; $n = 4$ for each point. (*B*) Altered KCNQ2 protein expression ratio in primary hippocampal neurons transfected with miR-106b-5p mimic or inhibitor. Rat hippocampal neurons at DIV2 were transfected with 50 nM scramble or miR-106b-5p of either mimic or inhibitor and harvested at DIV7 for KCNQ2 protein assessment. The ratio between KCNQ2 and α-tubulin levels was presented on the bottom. Data are mean ± SEM; $n = 3$ for each point. (*C*) Repressive effects of miR-17-5p, miR-20a-5p, or miR-93-5p mimic on native KCNQ2 protein levels in rat hippocampal neurons. The ratio between KCNQ2 and α-tubulin in cells transfected with 50 nM scramble or miRNA mimics was presented. Data are mean ± SEM; $n = 3$ to 4. $^*P < 0.05$, $^{**}P < 0.01$, one-way ANOVA followed by Šidák's post hoc test. ns, not significant.

(Fig. 3 *C*, *Bottom*), implying a strong posttranscriptional regulation of KCNQ2 protein synthesis.

In order to confirm that the developmental elevation of KCNQ2 protein level in early stages mediates the increase in M-type KCNQ channel activities, we measured KCNQ currents in primary cultured hippocampal neurons using voltage clamp electrophysiology. As shown in Fig. 3 *D*, *Top*, the amplitudes of outward K^+ currents gradually increased during early development. Tail current analysis of the K^+ current in the absence or presence of 10 μM XE991 at different DIV hippocampal neurons revealed a significant increase in XE991-sensitive KCNQ current between DIV5 and 15 (Fig. 3 *D*, *Bottom* and Fig. 3*E*). During the early developmental period, the cell capacitance also increased steadily due to increase in cell size (Fig. 3*F*). The results indicate that not only KCNQ2 protein expression but also slowly deactivating KCNQ channel activity were developmentally elevated at early postnatal stages in the rodent hippocampus.

The miR-106b Family Modulates KCNQ2 Expression in Early Hippocampal Development. In order to further investigate whether miR-106b family members are directly involved in the regulation of KCNQ channel expression in early developmental neurons, we tested the effects of removal of endogenous miRNAs by constructing a plasmid pU6-TuD-miR-106b-CMV-GFP (TuD-miR-106b), in which Tough Decoy (TuD) miR-106b-5p is expressed under a U6 promoter to ensure specific and stable knockdown of miR-106b-5p and a green fluorescent protein (GFP) gene is expressed under a human cytomegalovirus (CMV) promoter to permit visualization in single neurons. The

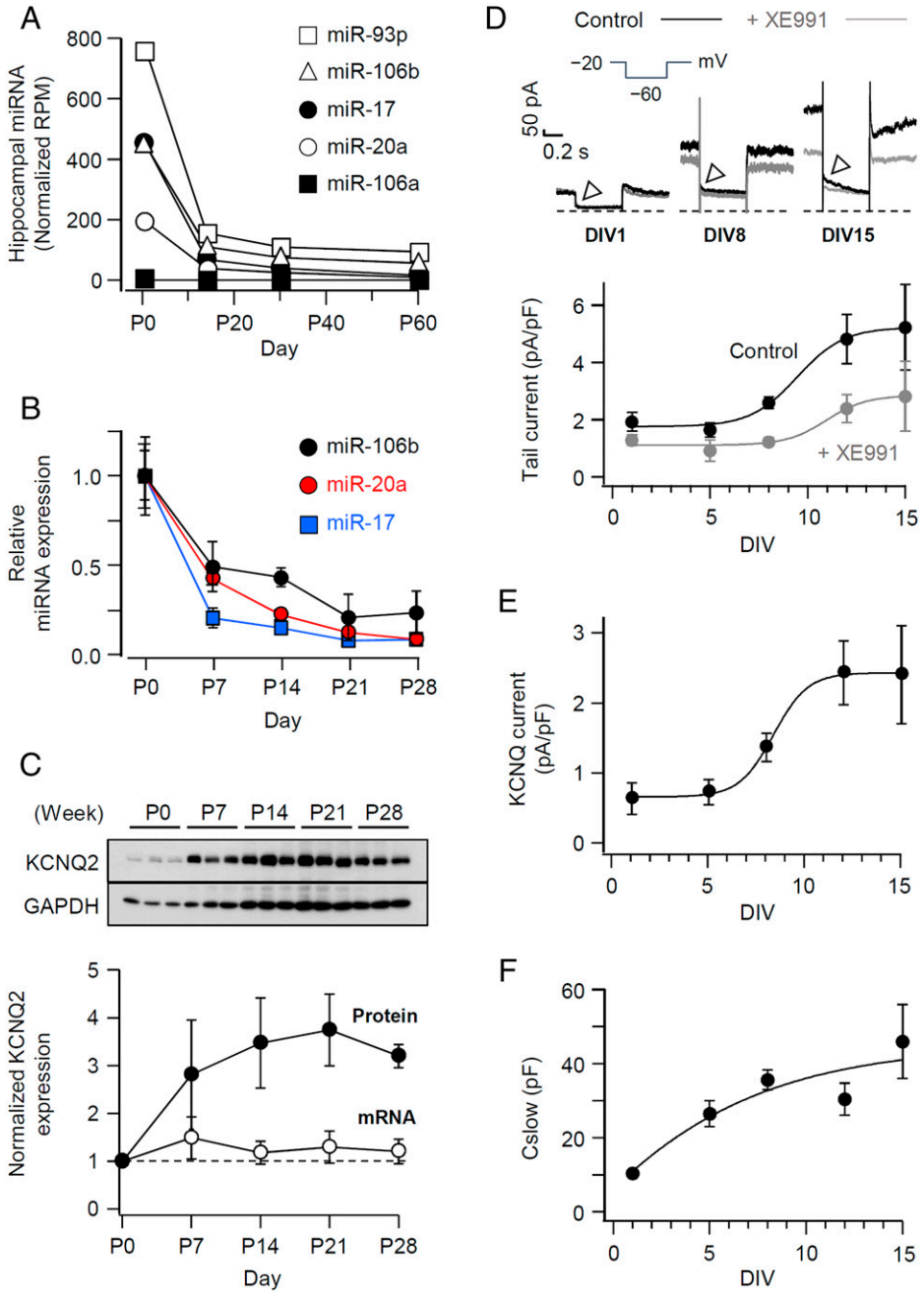

Fig. 3. Developmentally regulated miR-106b family members control the expression of KCNQ2 proteins in the rodent hippocampus. (*A*) Time-dependent changes in the levels of miR-106b-5p family miRNAs. Normalized RPM levels for miR-17-5p, miR-20a-5p, miR-93-5p, miR-106a-5p, and miR-106b-5p were measured in mouse hippocampi harvested at P0, P14, P30, and P60 stages. Note that miR-106a-5p was not detectable throughout these stages. (*B*) Real-time PCR analysis of miR-106b-5p expression level in mouse hippocampal tissues isolated from P0, P7, P14, P21 and P28. Each point was obtained from three mice, and the mean miRNA value at P0 was scaled to 1. Data are mean ± SEM. (*C*) Differential expression patterns of KCNQ2 mRNA and protein levels during early development (P0 through P28) in mouse hippocampi. Western blot analyses of KCNQ2 and GAPDH at five different stages in three mice per condition each day. (*Bottom*) Relative expression levels of KCNQ2 mRNA and protein in the hippocampus were normalized to GAPDH mRNA and protein, respectively. All data are mean ± SEM; $n = 6$ mice for each stage. (*D*) Time-dependent increase in tail current density in cultured dissociated neurons. (*Top*) Representative traces of native $K^{\pm}$ currents measured at three different time points (DIV) with or without XE991 (10 μM) in cultured rat primary hippocampal neurons. DIV1 corresponds to P0, as the neurons were isolated from rat embryos on E18. Arrowhead indicates the tail current. Inset indicates pulse protocol. (*Bottom*) Tail current densities in neurons with or without XE991 were obtained by dividing the peak amplitudes of tail currents (pA) by cell capacitances (pF). All data are mean ± SEM; $n = 6$ to 8 for each time point. (*E*) Time-dependent increase in KCNQ-selective current density. KCNQ current density was obtained by subtracting XE991-insensitive tail current density from the total tail current density in each neuron. (*F*) Time-dependent changes in cell capacitance in cultured dissociated neurons.

TuD-miR-106b construct is designed to have two miR-106b binding sites flanked by a stem and a stem loop bulged structure, which allows long-term and stable expression of miR-106b inhibitor by protecting against ribonuclease (RNase) attack in cells or tissues (Fig. 4*A*) (42). Conversely, in order to assess the impact of miR-106b up-regulation in neurons, we also developed a plasmid, pU6-precursor-miR-106b-CMV-GFP (precursor-miR-106b), that expresses precursor-miR-106b-5p under a U6

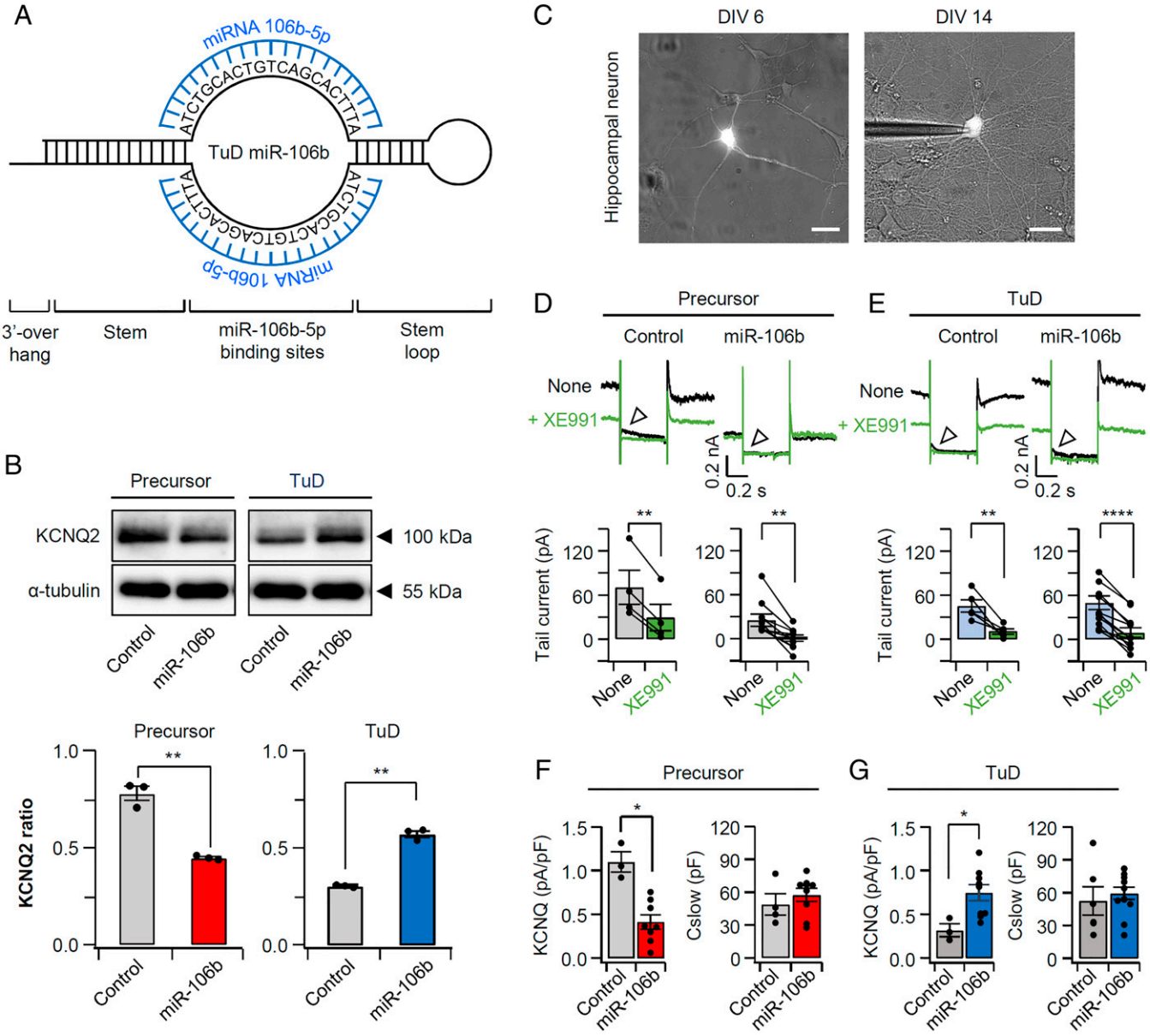

Fig. 4. Precursor-miR-106b-5p and TuD-miR-106b-5p lead to significant changes in KCNQ2 protein levels and concomitant M-currents in rat primary hippocampal neurons. (*A*) Structure of TuD-miR-106b-5p construct allowing efficient inhibition of miR-106b-5p. The plasmids for control and miR-106b-5p of precursor and TuD were constructed as described in *Materials and Methods*. (*B*, *Top*) KCNQ2 protein levels in cultured neurons transfected with precursor-miR-106b-5p (*Left*) or TuD-miR-106b-5p (*Right*). (*Bottom*) The ratio between KCNQ2 and α-tubulin in cells transfected with precursor-control or TuD control was compared with the ratio obtained from cells transfected with precursor-miR-106b-5p or TuD-miR-106b-5p, respectively. Data are mean ± SEM; $n = 3$ for each point. (*C*) sCMOS images of DIV6 and DIV14 primary hippocampal neurons expressing GFP. K^+ currents were recorded in hippocampal pyramidal neurons at DIV14 via whole-cell patching around the soma and AIS region. (*D*, *Top*) Representative traces of K^+ currents in hippocampal pyramidal neurons transfected with control or miR-106b-5p of precursor before (none, black) and after (green) addition of 10 μM XE991. (*Bottom*) Summary of tail K^+ current amplitudes before and after XE991 application in cells expressing precursor plasmids. Data are mean ± SEM ($n = 4$ to 6). $^{**}P < 0.01$, compare to none. (*E*, *Top*) Representative traces of K^+ currents in hippocampal pyramidal neurons transfected with control or miR-106b-5p of TuD before (none, black) and after (green) addition of 10 μM XE991. (*Bottom*) Summary of tail K^+ current amplitudes before and after XE991 application in cells expressing TuD plasmids. Data are mean ± SEM ($n = 5$ to 10). $^{**}P < 0.01$; $^{****}P < 0.0001$, compare to none. (*F*) XE991-sensitive KCNQ current densities in neurons transfected with control or miR-106b precursor. KCNQ currents were obtained by subtracting tail current amplitude after XE991 application from amplitudes recorded prior to XE991 application. Cslow (pF) represents cell capacitance of hippocampal neurons; there was no significant difference in Cslow between neurons expressing precursor-control and precursor-miR-106b. Data are mean ± SEM ($n = 4$ to 6). $^{*}P < 0.05$, compared to control. (*G*) XE991-sensitive KCNQ current densities in neurons transfected with control or miR-106b TuD. KCNQ currents were obtained by subtracting tail current amplitude after XE991 application from amplitude before XE991 application. There was no significant difference in Cslow between neurons expressing TuD control and TuD-miR-106b. Data are mean ± SEM ($n = 5$ to 10). $^{*}P < 0.05$, compared to control.

promoter and GFP under a CMV promoter. Precursor-miR-106b is processed to generate a functionally active and mature form of miR-106b-5p in cells. As shown in Fig. 4*B*, transfection of DIV2 neurons with precursor-miR-106b led to a significant decrease in KCNQ2 protein level compared to cells expressing precursor-control, while TuD-miR-106b robustly increased the KCNQ2 protein level compared to TuD control. These results demonstrate that miR-106b plays a critical role in the early

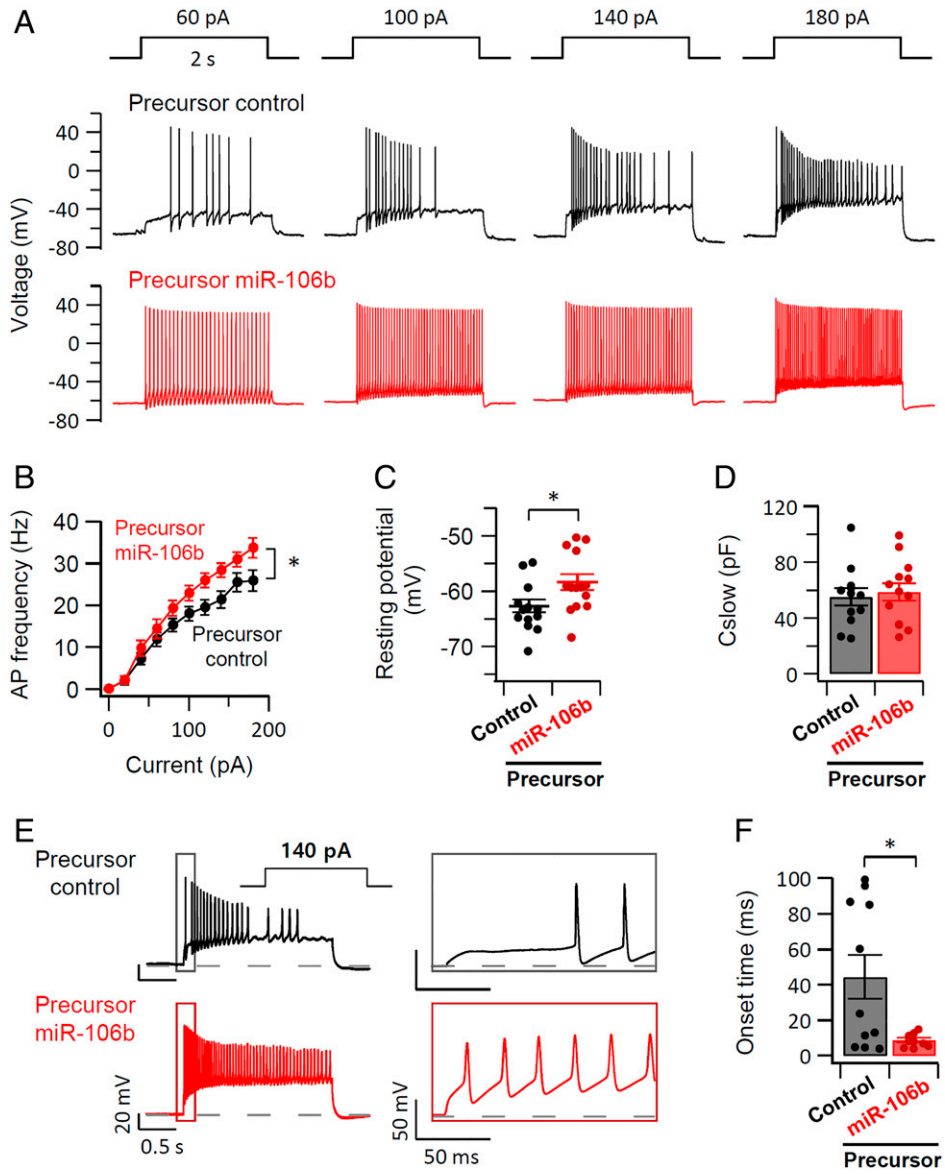

Fig. 5. Precursor-miR-106b-5p enhances membrane excitability in hippocampal pyramidal neurons. Rat hippocampal neurons at DIV2 were transfected with precursor or TuD plasmids and used at DIV7 for spike-frequency assessment. (*A*) Representative traces of spike trains in response to 2-s current injection steps from 0 to 180 pA were measured in neurons transfected with precursor-control (*Top*) and precursor-miR-106b-5p (*Bottom*). (*B*) Spike (AP) frequency induced by current pulses in neurons expressing precursor-control ($n = 12$) or precursor-miR-106b-5p ($n = 11$). *$P < 0.05$, determined by two-way repeated ANOVA. (*C*) Summary of resting potential at 0 pA in neurons expressing precursor-control ($n = 14$) or precursor-miR-106b-5p ($n = 14$). *$P < 0.05$, determined by Student's *t* test. (*D*) Cell capacitance was compared by measuring Cslow in hippocampal neurons expressing precursor plasmids. (*E*) Representative spike trains induced by a 140-pA current injection in neurons expressing precursor-control (*Left*) or precursor-miR-106b-5p (*Right*). Boxes show spike traces during the initial 150-ms current injection. (*F*) Summary of the onset time for AP generation in neurons expressing precursor-control ($n = 11$) or precursor-miR-106b-5p ($n = 11$). Data are mean ± SEM. *$P < 0.05$, compared to precursor-control.

developmental control of KCNQ2 protein expression in hippocampal neurons.

To further examine the effects of miR-106b manipulation on KCNQ channel expression, we measured the KCNQ K^+ current in hippocampal pyramidal neurons transfected with the plasmids for precursor-miR-106b or TuD-miR-106b. Neurons typically began to present GFP fluorescence within 2 d after transfection (Fig. 4*C*). When we measured K^+ currents in DIV14 hippocampal neurons transfected with plasmid precursor-control, the outward tail currents were significantly inhibited by the application of 10 μM XE991, a selective KCNQ channel inhibitor. The difference in magnitude of tail currents before and after XE991 application was defined as the M-current in the hippocampal neuron (Fig. 4 *D*, *Left*). In neurons transfected with plasmid precursor-miR-106b, the total outward tail currents significantly decreased and were inhibited by XE991 to a lesser extent (Fig. 4 *D*, *Right*). On the other hand, in cells expressing TuD-miR-106b, the amplitude of outward currents was increased and the tail current suppression by XE991 was much stronger compared to cells expressing TuD control (Fig. 4*E*). When we measured the differences in tail current amplitude before and after XE991 application, the KCNQ current density was lower in cells expressing precursor-miR-106b compared to precursor-control, while it was higher in cells expressing TuD-miR-106b (Figs. 4 *F* and *G*, *Left*). However, overexpression or knockdown of miR-106b did not cause any significant changes in the XE991-insensitive K^+ current densities (*SI Appendix*, Fig. S3), further suggesting that the

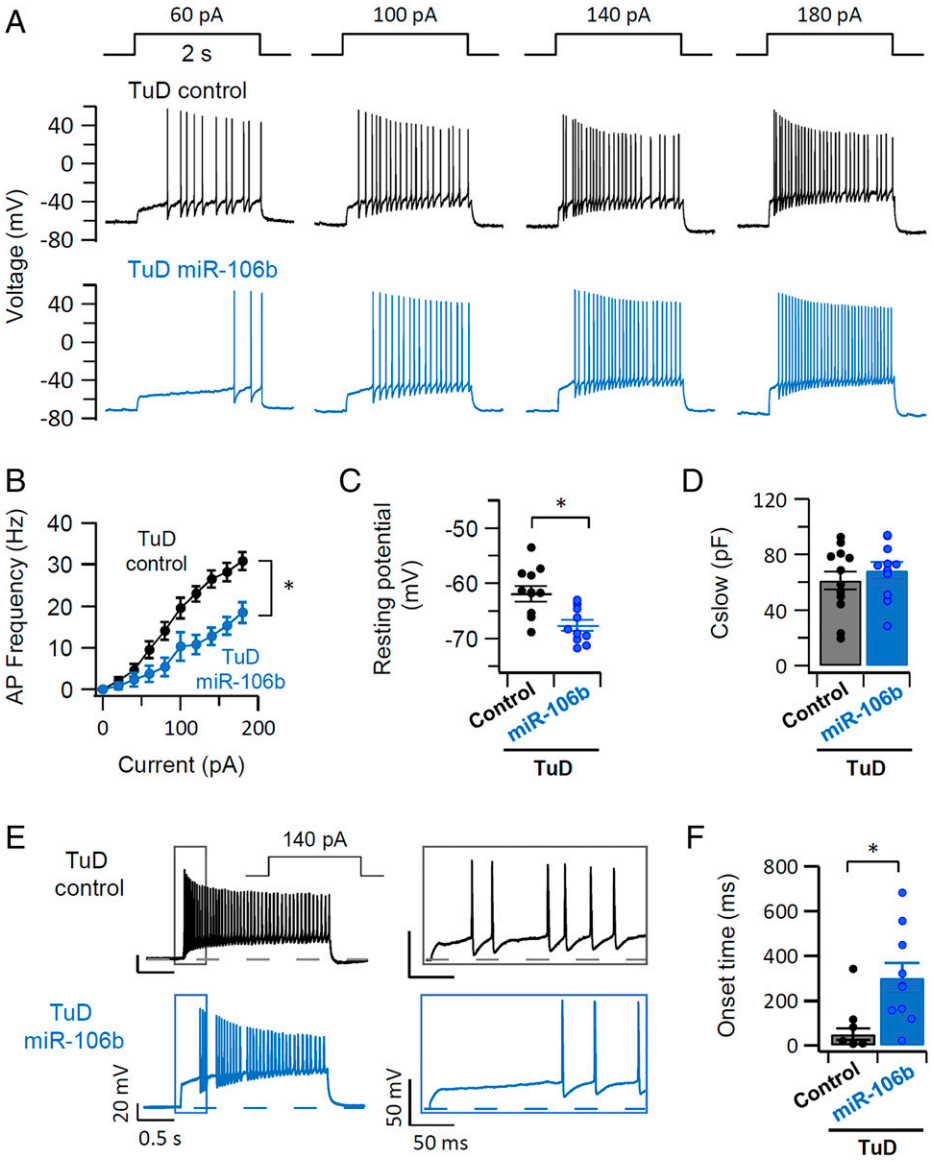

Fig. 6. TuD-miR-106b-5p suppresses cellular excitability and spike frequency in hippocampal pyramidal neurons. (*A*) Representative traces of spike trains in response to 2-s current injection steps from 0 to 180 pA were measured in neurons transfected with TuD control (*Top*) and TuD-miR-106b-5p (*Bottom*). (*B*) Spike (AP) frequency induced by current pulses in neurons expressing control or miR-106b-5p TuD plasmids. TuD control, $n = 13$ and TuD-miR-106b, $n = 13$. $^*P < 0.05$, determined by two-way repeated ANOVA. (*C*) Summary of resting potential at 0 pA in neurons expressing TuD control ($n = 13$) or TuD-miR-106b-5p ($n = 10$). $^*P < 0.05$, determined by Student's *t* test. (*D*) Cell capacitance was compared by measuring Cslow in hippocampal neurons expressing TuD plasmids. (*E*) Representative spike trains induced by a 140-pA current injection in neurons expressing TuD control (*Left*) or TuD-miR-106b-5p (*Right*). Boxes show spike traces during the initial 150-ms current injection. (*F*) Summary of onset time for AP generation in neurons expressing TuD control ($n = 13$) or TuD-miR-106b-5p ($n = 10$). Data are mean ± SEM. $^*P < 0.05$, compared to TuD control.

miRNA-induced K^+ current changes were due to the manipulation of M-type KCNQ current. Alterations of the miR-106b level did not affect the membrane capacitance (Cslow) (Figs. 4 *F* and *G*, *Right*). Together, these results indicate that miR-106b plays an important role in regulating M-type KCNQ channel expression in early hippocampal neurons.

Manipulation of miR-106b Level Affects Hippocampal Excitability. We next examined the effects of miR-106b up-regulation on membrane excitability in hippocampal neurons transfected with plasmids of precursor-control or precursor-miR-106b. To measure the excitability of hippocampal neurons, spike trains were recorded after injection of depolarizing currents ranging from 0 to 180 pA. Spontaneous electrical activity generated by the dynamic balancing of excitatory and inhibitory synaptic transmission was inhibited by fast synaptic transmission blockers (see *Materials and Methods*; ref. 43) (*SI Appendix*, Fig. S4). The hippocampal neurons transfected with precursor-control plasmid revealed typical patterns of neuronal firing, such as delay, adaptation, silence, and bursting (Fig. 5 *A*, *Top*) (44, 45). In neurons expressing precursor-miR-106b, however, the delayed and adapting spikes were weakened and the silences and bursting disappeared (Fig. 5 *A*, *Bottom*). In addition, the number of events during depolarization was significantly higher in cells transfected with precursor-miR-106b than those transfected with precursor-control, and the AP frequency difference was greater at higher current injections (Fig. 5*B*). The resting potential (−62.6 ± 1.1 mV) of hippocampal neurons

transfected with precursor-miR-106b was statistically lower than that (−58.4 ± 1.4 mV) of neurons transfected with precursor-control (Fig. 5*C*). Those differences were not attributable to alterations in the membrane surface properties of the hippocampal neurons, as there were no significant changes in surface area (Fig. 5*D*). The delayed firing response, which is measured as the first-spike latency after current injection, is a defining electrical property of hippocampal neurons. Our data show that the average delayed response was 44.5 ± 12.3 ms at 140 pA in cells transfected with precursor-control. This response was significantly reduced to 9.0 ± 1.2 ms in cells transfected with precursor-miR-106b (Fig. 5 *E* and *F*). The effects of precursor-miR-106b on AP firing was further characterized in a single AP generated by a short current injection. We observed that the maximum rate obtained from the first derivative of AP was reduced from 347 ± 23 mV/ms to 282 ± 15 mV/ms by expressing precursor-miR-106b, but half width and amplitude were not changed (*SI Appendix*, Fig. S5 *A–E*). Together, these data indicate that elevation of intracellular miR-106b levels using precursor plasmid increases neuronal excitability, likely by reducing KCNQ2 protein expression.

On the other hand, transfection of TuD-miR-106b into hippocampal neurons led to significantly reduced neuronal excitability and delayed firing responses compared to TuD control (Fig. 6*A*). TuD-miR-106b also significantly reduced AP frequency (Fig. 6*B*). The resting potential significantly decreased from −62.8 ± 1.5 mV to −67.6 ± 1.0 mV after transfection with TuD-miR-106b (Fig. 6*C*). However, TuD-miR-106b did not alter the capacitance of neurons (Fig. 6*D*). The average onset time for the first firing response was significantly increased from 49.6 ± 26.2 ms in TuD control to 302.9 ± 65.6 ms in TuD-miR-106b (Fig. 6 *E* and *F*). However, TuD-miR-106b did not alter other AP properties including half width, amplitudes, and phase plot of AP (*SI Appendix*, Fig. S5 *F–J*). These data indicate that TuD-miR-106b reduces neuronal excitability by knocking down endogenous miR-106b-5p, which in turn represses KCNQ2 expression.

miR-17 Mimics miR-106b in Regulating KCNQ Current and Neuronal Excitability. Although the miR-17 mimic was less efficient in limiting KCNQ2 protein levels compared to miR-106b (Fig. 2 *A* and *C*), it strongly suppressed the XE991-sensitive KCNQ tail currents in hippocampal neurons (*SI Appendix*, Fig. S6 *A–C*) and enhanced neuronal excitability and firing frequency by elevating the resting membrane potential (*SI Appendix*, Fig. S6 *D–F*). In addition, it slowed the initial onset time of AP generation by a 140-pA current injection (*SI Appendix*, Fig. S6*G*). When we performed similar experiments with more stable precursor-miR-17 and TuD-miR-17, the spike frequency, resting membrane potential, and AP onset time were all inversely regulated by the two plasmids in hippocampal neurons (see details in *SI Appendix*, Fig. S7). Finally, we confirmed that miR-17 expression similarly inhibited KCNQ currents in cortical pyramidal neurons (*SI Appendix*, Fig. S8), suggesting that the dynamic regulatory effects of the miR-106b family on KCNQ2 protein expression may be a general phenomenon across multiple brain tissue types.

Discussion

In this report, we have shown that select miR-106b family members are highly expressed in the rodent brain and play a functional role in regulating the expression of the KCNQ2 potassium channel during early developmental stages in hippocampal neurons by interacting with the 3′-UTR of KCNQ2 mRNA. Bioinformatic predictions of miRNAs that likely target KCNQ mRNA revealed a target site for the miR-106b family in the 3′-UTR of the KCNQ2 mRNA. However, the prediction did not yield any strong candidate binding sites for miRNAs in the other KCNQ mRNAs, including KCNQ1, KCNQ3, KCNQ4, and KCNQ5, suggesting that miR-106b expression may not change other M-currents (e.g., KCNQ3/5) in the hippocampal pyramidal neurons (46). Our bioinformatic prediction analyses also indicate that the regulatory effects of miR-106b on M-currents are conserved for KCNQ2 channel expression because the miR-106b target site was not found in other K^+ channels influencing the membrane excitability, such as Kv1.2 (KCNA2), Kv11.1 (erg), KCa1.1 (BK), Kir6.1 (KCNJ8), and Kir6.2 (KCNJ11). Through in vitro luciferase assays, we confirmed that three members of the miR-106 family, including miR-106b, miR-17, and miR-20a, repress KCNQ2 protein expression by binding to the same target site in the 3′-UTR of the KCNQ2 mRNA. In hippocampus, KCNQ2 protein levels and currents gradually increased during the first 3 wk of postnatal development, while the miRNA level of miR-106b family members gradually decreased over the same period. However, the level of KCNQ2 mRNA increased slightly within 1 wk and then stabilized throughout the following weeks, which is consistent with the previous reports (38). In our comparative studies examining hippocampal tissues sampled at time points ranging from P7 to P28, the expression levels of miR-106 family members continuously decreased while the KCNQ2 mRNA level remained steady, suggesting that miRNAs of the miR-106 family repress KCNQ2 protein synthesis by arresting the translation process rather than destabilizing the mRNA. Therefore, the high levels of miR-106b family miRNAs that we observed in the newborn hippocampus may contribute to the low level of KCNQ2 proteins in newborn neural tissue. Likewise, the gradual decline in expression of KCNQ2 from P0 to P28 may boost KCNQ2 protein recovery through derepression. This inverse correlation in expression levels between miR-106b family miRNAs and KCNQ2 protein suggests that relief from translational repression by miRNAs is the primary mechanistic driver of early developmental elevation of KCNQ channel activity in the infant brain.

miRNAs belonging to the broad miR-106b family are derived from the highly conserved miR-106b~25 and miR-17~92 miRNA clusters located on chromosomes 7 and 13, respectively (40, 47). They show similar patterns of tissue distribution, expression levels, and partially overlapping functions in animal development (48). Notably, they are abundantly expressed in cancer cells and promote cell migration and metastasis of carcinoma cells (48, 49). Several recent studies have shown that miR-106b is up-regulated in the brains of epileptic patients, and thus miR-106b was indicated as a highly sensitive and specific diagnostic marker for epilepsy (12–15). Here, we found that miR-106 family members are highly expressed in early developing hippocampal neurons and that the expression of these miRNAs dramatically decreases over several weeks after birth. Ectopic expression of precursor-miR-106b prevents normal KCNQ2 protein synthesis and elevates resting membrane potential and neuronal excitability, suggesting that up-regulation of miR-106b may precipitate epileptic phenotypes in patients by reducing KCNQ channel activity in neurons. Our data demonstrate that the high levels of miR-106b family members observed during the embryonic stage may contribute to the early proliferation of hippocampal neurons during embryonic development and that the gradual decline of miR-106 family members after birth may foster neuronal differentiation and developmental maturation of hippocampal neurons by elevating KCNQ channel activity.

Each miR-106b family member has the potential to repress translational expression by binding to the same target site on the 3′-UTR of KCNQ2 mRNA. However, our data suggest that the conserved seven-nucleotide target sequence is insufficient to fully drive the translational regulation of KCNQ2 mRNA. Notably, we did not observe significant effects of miR-93 overexpression on

luciferase activity in HEK293T cells nor in Western blot experiments in the primary hippocampus. This inconsistent repressive potential among different members of the miR-106b family might come from their differential binding affinities for the target site within the KCNQ2 mRNA. miR-93 has three possible extra interactions beyond the specific conserved interactions between the miRNA and its target mRNA, whereas other miR-106b family members have five to six extra possible interactions. This difference may account for the relative inefficiency of miR-93 in targeting the KCNQ2 transcript and regulating its expression. Similar findings were also reported in previous studies. Wahlquist et al. (50) reported that miRNA family members miR-25 and miR-92a share the same seed sequences but that only miR-25 could regulate expression of SERCA2 protein in human cardiomyocytes. A more recent work showed that seed pairing is not always sufficient for functional target interaction and that additional base pairing to the 3′ end of miRNA beyond the seed sequence is required for specific targeting by miRNA family members (41). Since additional interactions around the seed sequence are needed for stable and high-affinity interaction between miRNAs and mRNA, down-regulation of certain miRNAs is enough for changing the phenotype despite the presence of other family members (51).

Depolarization dramatically changes the firing patterns in hippocampal neurons (44, 45, 52). Importantly, the M-type KCNQ2/3 channel is known to play a key role in controlling firing patterns, such as burst generation, after depolarization in neurons (24). Malfunction of KCNQ2/3 channels leads to benign familial neonatal convulsion, a rare autosomal-dominant idiopathic epilepsy in newborns. The epilepsy is characterized by the occurrence of focal or generalized tonic-chronic convulsions starting around day 3 of life and spontaneously disappearing within 1 to 4 mo (53, 54). While both the KCNQ2 and KCNQ3 subunits comprise the active heteromeric M-channels, previous studies established that M-channel activity and neuronal excitability are particularly sensitive to variations in KCNQ2 subunit expression (30). Moreover, knockout of KCNQ2, but not KCNQ3, in hippocampal pyramidal neurons eliminated M-channel function at the cellular level (24, 25, 27, 55). We found here that reduction of KCNQ2 levels resulting from the expression of precursor-miR-106b was sufficient to trigger a decrease in spike adaptation and silence and to increase neuronal excitability, whereas the elevation of KCNQ2 levels by TuD-miR-106b increased spike adaptation and silence and decreased membrane excitability (56). Our data also showed that reduction of KCNQ2 protein by precursor-miR-106b almost completely eliminated first-spike latency, while elevation of the KCNQ2 level by Tud-miR-106b significantly increased latency in hippocampal neurons. We also observed that the expression of precursor-miR-106b, but not TuD-miR-106b, decreased AP maximal rise. This selectivity can be attributed to the differential regulation of sodium channel activity in the plasma membrane. Previous studies have reported that reduction of KCNQ2 expression led to the increase of sodium channel inactivation (57, 58). The inhibitory effect of precursor-miR-106b expression on AP maximal rise could be interpreted as the results of sodium channel inactivation by resting membrane potential increase following the reduction of KCNQ2 levels. These data indicate that physiological changes in the levels of miR-106 family miRNAs play a key role in modulating the excitability of neurons through the posttranslational regulation of the KCNQ2 channel proteins. However, it is unclear yet how manipulation of miR-106b miRNAs affects the molecular composition of M-channels in neurons. For example, experimental miR-106b reduction will increase the expression level of the KCNQ2 subunit and probably elevate the portion of KCNQ2 homomers or heteromers with 3:1 KCNQ2:KCNQ3 stoichiometry in the plasma membrane. Further studies will elucidate the modulatory effects of miR-106b on the molecular stoichiometry of M-channels.

Although we focused here on the functional role of the miR-106b–responsive target site located in the 3′-UTR region of rodent KCNQ2 genes, the target sequence also exists in either CDS alone or both 3′-UTR and CDS regions of KCNQ2 from certain vertebrates (Fig. 1*E*). From an evolutionary standpoint, the high conservation of the miR-106b target sequence in the CDS of KCNQ2 may relate to its functional significance, which could lead to purifying selection. The target sequence in the CDS could be maintained either for its role in protein function or its regulatory role in controlling gene expression level by permitting miRNA interactions. While the target sequence in the CDS is prevalent and the surrounding sequence is highly conserved in vertebrates, the target sequence in the 3′-UTR region only occurs in certain vertebrates. This implies that the finely tuned regulatory actions exerted on KCNQ2 via targeting of miRNAs to the 3′-UTR of KCNQ2 mRNA have arisen independently over the long course of vertebrate evolution. Most CDS regions targeted by miRNA are involved in regulating gene expression at the translational level (3, 59). This specialized kind of gene regulation also operates by a very unusual mechanism wherein unconventional miRNA recognition elements are used (60). The targeting of miR-20-5p to the CDS of DAPK3, in this example, does not involve conventional 5′ seed–base pairings but instead relies on extensive base pairings at the 3′ end. Through these unusual interactions at the CDS of DAPK3, miR-20-5p down-regulates DAPK3 translation without affecting mRNA stability. Whether miRNA target sites in the CDS are involved in the regulation of KCNQ2 expression and whether there are unconventional miRNA recognition elements in the CDS of KCNQ2 remain to be studied in depth.

Materials and Methods

Animals and Tissue Collection. Male mice (C57BL/6J strain) and Sprague Dawley rats at specific postnatal stages were obtained from the Korea Research Institute of Bioscience and Biotechnology-Institutional Animal Care and Use Committee. All animals were maintained under "specific pathogen-free" conditions. Mice and rats without visible signs of disease were killed, and their hippocampal tissues were immediately dissected and flash-frozen in liquid nitrogen. Both hippocampi from each rodent were obtained for a single animal sample. Those tissues were used for Western blot analysis and total RNA extraction.

Cell Culture and Transfection. HEK-293T (tsA-201) cells were cultured at 37 °C under 5% (vol/vol) CO_2 in Dulbecco's modified Eagle's medium (Lonza) supplemented with 5% fetal calf serum (Sigma-Aldrich), penicillin (100 U/mL), and streptomycin (0.1 mg/mL) (Sigma-Aldrich). Dissociated hippocampal neurons from WT rat pups (E18) were plated on poly-L-lysine–coated glass coverslips (18 mm; Bellco Glass) in 12-well plates (culture area: 3.38 cm^2) in a volume of 1 mL per well and were maintained in neurobasal medium supplemented with B27 (Invitrogen), glutamine (Sigma-Aldrich), and penicillin/streptomycin. The cultured neurons were transfected at DIV2 using the CalPhos Mammalian Transfection Kit (Clontech, Takara Bio).

Plasmid Construction. For construction of TuD-miR-106b-5p plasmid, DNA sequences (5′AAGGATCCGACGGCGCTAGGATCATCAACATCTGCACTGTCAGCACTTTACAAGTATTCTGGTCACAGAATACAACATCTGCACTGTCAGCACTTTACAAGATGATCCTAGCGCCGTCTTTTTTGGAAAAGCTTAA3′) containing stem, stem loop, and two miR-106b-5p binding sites flanked by BamH1/HindIII sites were synthesized and cloned into BamH1/HindIII sites of pmiENSR (a gift from Eunmi Hwang, Korea Institute of Science and Technology, Seoul, Korea) plasmid, where U6 promoter drives expression of small RNA efficiently. DNA sequences (5′AAGGATCCGACGGCGCTAGGATCATCAACGGTTCGTACGTACACTGTTCACAAGTATTCTGGTCACAGAATACAACGGTTCGTACGTACACTGTTCACAAGATGATCCTAGCGCCGTCTTTTTTGGAAAAGCTTAA3′) containing stem, stem loop, and two *Arabidopsis* miR-416 binding sites flanked by BamH1/HindIII sites were generated for TuD control plasmid construction to serve as a nonspecific control. The miR-106b-5p expression plasmid, precursor-miR-106b-5p, was constructed by synthesis of the DNA sequence of stem and loop sequence (5′AAGGATCCCCTGCTGGGACTAAAGTGCTGACAGTGCAGATAGTGGTCCTCTCTGTGCTACCGCACTGTGGGTACTTGCTGCTCCAGCAGGAAGCTTAA3′) of mmu-miR-106b-5p and subsequent insertion into BamH1

and HindIII-digested pmiENSR. Stem and loop sequence (5′AAGGATCCGCG AAACTGAACCCGGTTTGTACGTATGGACCGCGTCGTTGGAATCCAAAAGAACC AGGTTCGTACGTACACTGTTCATCGTTTTTTGGAAAAGCTTAA3′) of *Arabidopsis* miR-416 was used for the precursor-control plasmid.

RNA Extraction and Real-Time PCR Assays for miRNA and mRNA. Total RNA was extracted from the mouse hippocampus tissues at ages of 1, 2, 3, 4, 5, and 6 wk with TRIzol Reagent (Invitrogen). Reverse transcription reactions were performed with the SuperScript First Strand complementary DNA (cDNA) synthesis system (Invitrogen) according to the manufacturer's instructions. Real-time PCR was performed with the One Step SYBR® PrimeScript™ RT-PCR Kit II (Takara Bio Inc.). The specific real-time PCR primers for miR-17-5p, miR-20a-5p, miR-93-5p, miR-106b-5p, U6, KCNQ2, and GAPDH were purchased from Bioneer. U6 and GAPDH served as internal controls for miRNA and mRNA assays, respectively. The cycle threshold (Ct value) was acquired using the Opticon Monitor Analysis Software (MJ Research). The data were analyzed using the 2-ΔΔCt method, and the values were presented by relative quantity.

miRNA Extraction and cDNA Library Construction. Small RNA was extracted using the Pure Link Microto-Midi total RNA Purification System kit (Invitrogen) and miRNeasy mini kit (Qiagen). A total of 10 μg small RNA per gel lane was subjected to electrophoresis through a 15% Tris-Borate-Ethylene-diamine-tetraacetic acid (TBE)-urea polyacrylamide gel electrophoresis (PAGE) gel. The fractions of the lanes containing RNA molecules between 18 and 30 nucleotides in length were excised. The small RNAs isolated from the gel slices were then attached with 5′ and 3′ adapters and were reverse transcribed using the Illumina Truseq kit (Illumina). The resulting cDNAs were amplified by PCR using Illumina primers and were then subjected to PAGE. The fractions of the lanes containing cDNA molecules between 60 and 80 nucleotides in length were excised for RNA extraction.

Small RNA Sequencing. The small RNA sample libraries were subjected to single-end sequencing with a read length of 50 nucleotides. The resulting raw sequences were mapped against the reference mouse genome (Mus_musculus; NCBIM37.55) using the software programs Cufflinks and TopHat (Johns Hopkins University). The number of sequence reads that corresponded to known miRNAs was determined by perfect sequence matching to the database of known miRNAs (miR Base release version 16, https://www.mirbase.org/). Raw data (the reads for each miRNA) were normalized to the total reads from each individual sample (*SI Appendix*, Table S1).

Dissection and Dissociation of Primary Hippocampal Neurons. Rat hippocampal neurons were isolated from embryonic day 18 (E18) animals and cultured for in vitro transfection and/or electrophysiological experiments. The hippocampi of E18 consist of major pyramidal neurons and a few glial cells. About 20 hippocampi were dissected from the brains under a stereoscopic microscope using two pairs of fine tweezers. The meninges were carefully removed from the hippocampi. After dissection, the hippocampi were washed gently with 7 to 8 mL Hanks' Balanced Salt Solution (HBSS) without Ca^{2+} and Mg^{2+} (HBSS, Invitrogen) in a 15-mL conical tube three times. After washing, 5 mL trypsin solution was added to the hippocampi in the tube, which were then incubated at 37 °C for 20 min. After incubation and digestion with the enzymes, hippocampi were slowly pipetted using a glass Pasteur pipette 12 times and then filtered using a wetted cell strainer (40-μm mesh, Falcon, Corning) into a 50-mL conical tube. Next, the supernatant was aspirated, and the pellet was resuspended in neurobasal medium supplemented with B27 (Invitrogen), glutamine (Sigma-Aldrich), and penicillin/streptomycin at a constant cell density of 4×10^4 cells/mL.

Luciferase Reporter Assays. Sequences of segments with a WT 3′-UTR region of KCNQ2 mRNA containing the predicted miR-17-5p/miR-20a-5p/miR-93-5p/miR-106b-5p binding sequences or mutant 3′-UTR were PCR amplified and cloned into the pGL3 luciferase reporter vector. All constructs were verified by sequencing. First, the HEK293T cells were seeded at 0.5×10^5 cells per well in 24-well plates 24 h prior to transfection. The following day, the pGL3 vector containing WT 3′-UTR of KCNQ2 mRNA or mutant (mut) 3′-UTR was cotransfected with either miR-17-5p, miR-20a-5p, miR-93-5p, miR-106b-5p mimics, or negative control into the cells. After 48 h, all cells were harvested according to the manufacturer's protocol (Promega), and the Firefly and Renilla luciferase activity were determined using the dual-luciferase reporter assay system (Promega) with a Victor X machine (PerkinElmer). Firefly luciferase activity was normalized to Renilla luciferase activity. Three independent experiments were performed in triplicate.

Western Blot Analysis. Rat primary cultured hippocampal neurons were transfected with the plasmids at DIV2 and cultured until DIV7. The neurons were then placed on ice and rinsed twice with ice-cold phosphate buffered saline (PBS). The cells were then washed again with PBS and incubated at 4 °C for 10 min with agitation in radio-immunoprecipitation assay (RIPA) buffer containing protease inhibitors. The cells were lysed by brief sonication and centrifuged at 15,900 × *g* for 15 min at 4 °C. The total protein concentration was measured in diluted aliquots of the cell lysate (1:9 in fresh RIPA buffer). The protein concentration was determined by the bicinchoninic acid (BCA) reagent method. Samples (20 μg protein) were subjected to sodium dodecyl sulfate PAGE. Separated proteins on the gel were transferred onto polyvinylidene fluoride (PVDF) membranes (Roche Diagnostics). Blots were blocked with 5% fat-free dry milk for 1 h and then incubated overnight at 4 °C with indicated primary antibodies including rabbit anti-KCNQ2 and α-tubulin polyclonal antibody (Santa Cruz Biotechnology, diluted 1:500). Subsequently, the blots were incubated with horseradish peroxidase–conjugated secondary antibodies (Cell Signaling Technology, Inc., diluted 1:6,000) for 1 h. The immunoblot on the membrane was visible after developing with an enhanced chemiluminescence detection system, and results were analyzed with NIH Image 1.41 software.

Electrophysiological Recordings. M-type KCNQ currents were recorded at the AIS regions of visually identified rat hippocampal pyramidal neurons showing GFP fluorescence in whole-cell configurations using a HEKA EPC-10 patch-clamp amplifier with PatchMaster software (HEKA Elektronik). For analysis, Fit Master software was also used. Primary cultured neurons transfected with plasmids at DIV2 were incubated and used at the indicated time. Patch pipettes were pulled from borosilicate glass micropipette capillaries (1.5-mm outer diameter, 1.10-mm inner diameter, and 10-cm length; Sutter Instrument Co.) using a Flaming/Brown microscope puller model P-97 (Sutter Instrument Co.) and had resistances of 2 to 4 MΩ when filled with internal solution. Series-resistance errors were compensated at >60%, and fast and slow capacitance was compensated for before the applied test pulse sequences. Usually, we measured the amplitude of M-current from tail current at –50 mV after a depolarizing voltage step to –20 mV. The changes in tail current were obtained by taking the difference between the average current of the first 10 to 20 ms and the average current of the last 100 ms during the voltage step. Spike trains of APs in neurons transfected with precursor or TuD plasmids were evoked by injecting 2-s depolarizing current pulses of different intensities (0 to 180 pA) into the cells. Resting potential of the cells was obtained by measuring the average membrane voltages for 200 ms at 0 pA injection. K^+ currents were sampled at 10 kHz and filtered at 3 kHz. All recordings were leak and capacitance subtracted before analysis by use of a –P/5 protocol. The pipette solution for whole-cell patch clamp consisted of the following: 175 mM KCl, 5 mM $Mgcl_2$, 0.1 mM BAPTA, 3 mM Na_2ATP, and 0.1 mM Na_3GTP, adjusted pH 7.4 with KOH and osmolality of 321 to 350 mOsm. The Ringer's solution for extracellular solution consisted of the following: 160 mM NaCl, 2.5 mM KCl, 2 mM $CaCl_2$, 1 mM $MgCl_2$, 10 mM Hepes, and 8 mM glucose, adjusted to pH 7.4 with NaOH and osmolality of 321 to 350 mOsm. A total of 4 μM 6-cyano-7-nitroquinoxaline-2,3-dione, 100 μM picrotoxin, and 25 μM D-2-amino-5-phosphonovaleric acid were added to the extracellular solution to block α-amino-3-hydroxy-5-methyl-4-isoxazole propionic acid (AMPA)-mediated, gamma-aminobutyric acid (GABA)-mediated, and N-methyl-D-aspartate (NMDA)-mediated synaptic transmission, respectively. The reagents were as follows: BAPTA, Na_2ATP, and Na_3GTP (Sigma-Aldrich) and other chemicals (Merck).

Image Acquisition. The optical imaging setup was built from an inverted microscope (Eclipse Ti, Nikon Instuments). A white light emitting diode (LED) light (TouchBright X3, Live Cell Instrument) was applied for exciting fluorescence. The excitation and emission lights were filtered using a GFP dichroic filter set (Brightline florescence filter) and collected on a Zyla sCMOS 5.5 camera (Andor Technologies). The sCMOS exposure time was 34 ms, and frames were 2,560 × 2,160 pixels with 16 bits per pixel. The camera was controlled by micromanager open source software, and images were acquired by ImageJ software (NIH).

Statistical Analysis. All data were analyzed using Excel 2016 (Microsoft), IGOR Pro-6.34, and GraphPad Prism 7 (GraphPad Software). Statistics in text or figures represent mean ± SEM. Statistical comparisons were made by two-way ANOVA repeated measures and Student's *t* test depending on the number of experimental groups. Data for time (age)-dependent current density, AP number–current curve, and AP frequency–current curve were fitted by Boltzmann function.

Data Availability. All study data are included in the article and/or *SI Appendix*.

ACKNOWLEDGMENTS. We thank many laboratories for providing the plasmids. This work was supported by grants from the National Research Foundation of Korea, a grant funded by the Korean government (Ministry of Science, Information and Communications Technology, and Future Planning, No. 2019R1A2B5B01070546), and the Basic Science Research Program (No. 2020R1A4A1019436).

1. V. Ambros, The functions of animal microRNAs. *Nature* **431**, 350–355 (2004).
2. E. Huntzinger, E. Izaurralde, Gene silencing by microRNAs: Contributions of translational repression and mRNA decay. *Nat. Rev. Genet.* **12**, 99–110 (2011).
3. J. Hausser, A. P. Syed, B. Bilen, M. Zavolan, Analysis of CDS-located miRNA target sites suggests that they can effectively inhibit translation. *Genome Res.* **23**, 604–615 (2013).
4. A. M. Krichevsky, K. S. King, C. P. Donahue, K. Khrapko, K. S. Kosik, A microRNA array reveals extensive regulation of microRNAs during brain development. *RNA* **9**, 1274–1281 (2003).
5. M. Somel *et al.*, MicroRNA-driven developmental remodeling in the brain distinguishes humans from other primates. *PLoS Biol.* **9**, e1001214 (2011).
6. A. J. Giraldez *et al.*, MicroRNAs regulate brain morphogenesis in zebrafish. *Science* **308**, 833–838 (2005).
7. D. De Pietri Tonelli *et al.*, miRNAs are essential for survival and differentiation of newborn neurons but not for expansion of neural progenitors during early neurogenesis in the mouse embryonic neocortex. *Development* **135**, 3911–3921 (2008).
8. G. P. Brennan, D. C. Henshall, MicroRNAs in the pathophysiology of epilepsy. *Neurosci. Lett.* **667**, 47–52 (2018).
9. Y. Ma, The challenge of microRNA as a biomarker of epilepsy. *Curr. Neuropharmacol.* **16**, 37–42 (2018).
10. C. Gross *et al.*, MicroRNA-mediated downregulation of the potassium channel KV4.2 contributes to seizure onset. *Cell Rep.* **17**, 37–45 (2016).
11. C. Gross, D. Tiwari, Regulation of ion channels by microRNAs and the implication for epilepsy. *Curr. Neurol. Neurosci. Rep.* **18**, 60 (2018).
12. N. An, W. Zhao, Y. Liu, X. Yang, P. Chen, Elevated serum miR-106b and miR-146a in patients with focal and generalized epilepsy. *Epilepsy Res.* **127**, 311–316 (2016).
13. J. Zhao *et al.*, Efficacy of levetiracetam combined with sodium valproate on pediatric epilepsy and its effect on serum miR-106b in children. *Exp. Ther. Med.* **18**, 4436–4442 (2019).
14. J. Wang *et al.*, Genome-wide circulating microRNA expression profiling indicates biomarkers for epilepsy. *Sci. Rep.* **5**, 9522 (2015).
15. H. G. Elnady *et al.*, MicroRNAs as potential biomarkers for childhood epilepsy. *Open Access Maced. J. Med. Sci.* **7**, 3965–3969 (2019).
16. D. A. Brown, P. R. Adams, Muscarinic suppression of a novel voltage-sensitive K^+ current in a vertebrate neurone. *Nature* **283**, 673–676 (1980).
17. H.-S. Wang *et al.*, KCNQ2 and KCNQ3 potassium channel subunits: Molecular correlates of the M-channel. *Science* **282**, 1890–1893 (1998).
18. E. C. Cooper *et al.*, Colocalization and coassembly of two human brain M-type potassium channel subunits that are mutated in epilepsy. *Proc. Natl. Acad. Sci. U.S.A.* **97**, 4914–4919 (2000).
19. B. C. Suh, B. Hille, Recovery from muscarinic modulation of M current channels requires phosphatidylinositol 4,5-bisphosphate synthesis. *Neuron* **35**, 507–520 (2002).
20. E. C. Cooper, E. Harrington, Y. N. Jan, L. Y. Jan, M channel KCNQ2 subunits are localized to key sites for control of neuronal network oscillations and synchronization in mouse brain. *J. Neurosci.* **21**, 9529–9540 (2001).
21. J. J. Devaux, K. A. Kleopa, E. C. Cooper, S. S. Scherer, KCNQ2 is a nodal K^+ channel. *J. Neurosci.* **24**, 1236–1244 (2004).
22. D. V. Madison, R. A. Nicoll, Control of the repetitive discharge of rat CA 1 pyramidal neurones in vitro. *J. Physiol.* **354**, 319–331 (1984).
23. J. F. Storm, An after-hyperpolarization of medium duration in rat hippocampal pyramidal cells. *J. Physiol.* **409**, 171–190 (1989).
24. C. Yue, Y. Yaari, KCNQ/M channels control spike afterdepolarization and burst generation in hippocampal neurons. *J. Neurosci.* **24**, 4614–4624 (2004).
25. J. F. Otto, Y. Yang, W. N. Frankel, H. S. White, K. S. Wilcox, A spontaneous mutation involving Kcnq2 (Kv7.2) reduces M-current density and spike frequency adaptation in mouse CA1 neurons. *J. Neurosci.* **26**, 2053–2059 (2006).
26. B. C. Schroeder, C. Kubisch, V. Stein, T. J. Jentsch, Moderate loss of function of cyclic-AMP-modulated KCNQ2/KCNQ3 K^+ channels causes epilepsy. *Nature* **396**, 687–690 (1998).
27. H. C. Peters, H. Hu, O. Pongs, J. F. Storm, D. Isbrandt, Conditional transgenic suppression of M channels in mouse brain reveals functions in neuronal excitability, resonance and behavior. *Nat. Neurosci.* **8**, 51–60 (2005).
28. H. Watanabe *et al.*, Disruption of the epilepsy KCNQ2 gene results in neural hyperexcitability. *J. Neurochem.* **75**, 28–33 (2000).
29. A. V. Tzingounis, R. A. Nicoll, Contribution of KCNQ2 and KCNQ3 to the medium and slow afterhyperpolarization currents. *Proc. Natl. Acad. Sci. U.S.A.* **105**, 19974–19979 (2008).
30. H. Soh, R. Pant, J. J. LoTurco, A. V. Tzingounis, Conditional deletions of epilepsy-associated KCNQ2 and KCNQ3 channels from cerebral cortex cause differential effects on neuronal excitability. *J. Neurosci.* **34**, 5311–5321 (2014).
31. V. Barrese, J. B. Stott, I. A. Greenwood, KCNQ-encoded potassium channels as therapeutic targets. *Annu. Rev. Pharmacol. Toxicol.* **58**, 625–648 (2018).
32. T. Yu *et al.*, KCNQ2/3/5 channels in dorsal root ganglion neurons can be therapeutic targets of neuropathic pain in diabetic rats. *Mol. Pain* **14**, 1744806918793229 (2018).
33. F. A. Vigil, C. M. Carver, M. S. Shapiro, Pharmacological manipulation of KV7 channels as a new therapeutic tool for multiple brain disorders. *Front. Physiol.* **11**, 688 (2020).
34. J. S. Smith, C. A. Iannotti, P. Dargis, E. P. Christian, J. Aiyar, Differential expression of KCNQ2 splice variants: Implications to M current function during neuronal development. *J. Neurosci.* **21**, 1096–1103 (2001).
35. M. Okada *et al.*, Age-dependent modulation of hippocampal excitability by KCNQ-channels. *Epilepsy Res.* **53**, 81–94 (2003).
36. T. Kanaumi *et al.*, Developmental changes in KCNQ2 and KCNQ3 expression in human brain: Possible contribution to the age-dependent etiology of benign familial neonatal convulsions. *Brain Dev.* **30**, 362–369 (2008).
37. V. F. Safiulina, P. Zacchi, M. Taglialatela, Y. Yaari, E. Cherubini, Low expression of Kv7/M channels facilitates intrinsic and network bursting in the developing rat hippocampus. *J. Physiol.* **586**, 5437–5453 (2008).
38. N. Tinel, I. Lauritzen, C. Chouabe, M. Lazdunski, M. Borsotto, The KCNQ2 potassium channel: Splice variants, functional and developmental expression. Brain localization and comparison with KCNQ3. *FEBS Lett.* **438**, 171–176 (1998).
39. V. Telezhkin *et al.*, Kv7 channels are upregulated during striatal neuron development and promote maturation of human iPSC-derived neurons. *Pflugers Arch.* **470**, 1359–1376 (2018).
40. I. Ivanovska *et al.*, MicroRNAs in the miR-106b family regulate p21/CDKN1A and promote cell cycle progression. *Mol. Cell. Biol.* **28**, 2167–2174 (2008).
41. J. P. Broughton, M. T. Lovci, J. L. Huang, G. W. Yeo, A. E. Pasquinelli, Pairing beyond the seed supports microRNA targeting specificity. *Mol. Cell* **64**, 320–333 (2016).
42. T. Haraguchi, Y. Ozaki, H. Iba, Vectors expressing efficient RNA decoys achieve the long-term suppression of specific microRNA activity in mammalian cells. *Nucleic Acids Res.* **37**, e43 (2009).
43. A. Mazzoni *et al.*, On the dynamics of the spontaneous activity in neuronal networks. *PLoS One* **2**, e439 (2007).
44. C. B. Canto, M. P. Witter, Cellular properties of principal neurons in the rat entorhinal cortex. I. The lateral entorhinal cortex. *Hippocampus* **22**, 1256–1276 (2012).
45. P. Hemond *et al.*, Distinct classes of pyramidal cells exhibit mutually exclusive firing patterns in hippocampal area CA3b. *Hippocampus* **18**, 411–424 (2008).
46. M. Shah, M. Mistry, S. J. Marsh, D. A. Brown, P. Delmas, Molecular correlates of the M-current in cultured rat hippocampal neurons. *J. Physiol.* **544**, 29–37 (2002).
47. D. Mehlich, F. Garbicz, P. K. Włodarski, The emerging roles of the polycistronic miR-106b~25 cluster in cancer—A comprehensive review. *Biomed. Pharmacother.* **107**, 1183–1195 (2018).
48. A. Ventura *et al.*, Targeted deletion reveals essential and overlapping functions of the miR-17 through 92 family of miRNA clusters. *Cell* **132**, 875–886 (2008).
49. W. L. Yau *et al.*, Over-expression of miR-106b promotes cell migration and metastasis in hepatocellular carcinoma by activating epithelial-mesenchymal transition process. *PLoS One* **8**, e57882 (2013).
50. C. Wahlquist *et al.*, Inhibition of miR-25 improves cardiac contractility in the failing heart. *Nature* **508**, 531–535 (2014).
51. D. P. Bartel, Metazoan microRNAs. *Cell* **173**, 20–51 (2018).
52. J. Lübke, M. Frotscher, N. Spruston, Specialized electrophysiological properties of anatomically identified neurons in the hilar region of the rat fascia dentata. *J. Neurophysiol.* **79**, 1518–1534 (1998).
53. N. A. Singh *et al.*, Mouse models of human KCNQ2 and KCNQ3 mutations for benign familial neonatal convulsions show seizures and neuronal plasticity without synaptic reorganization. *J. Physiol.* **586**, 3405–3423 (2008).
54. C. Biervert *et al.*, A potassium channel mutation in neonatal human epilepsy. *Science* **279**, 403–406 (1998).
55. N. A. Singh *et al.*, A novel potassium channel gene, KCNQ2, is mutated in an inherited epilepsy of newborns. *Nat. Genet.* **18**, 25–29 (1998).
56. J. P. Cavaretta *et al.*, Polarized axonal surface expression of neuronal KCNQ potassium channels is regulated by calmodulin interaction with KCNQ2 subunit. *PLoS One* **9**, e103655 (2014).
57. Z. Niday, V. E. Hawkins, H. Soh, D. K. Mulkey, A. V. Tzingounis, Epilepsy-associated KCNQ2 channels regulate multiple intrinsic properties of layer 2/3 pyramidal neurons. *J. Neurosci.* **37**, 576–586 (2017).
58. A. Battefeld, B. T. Tran, J. Gavrilis, E. C. Cooper, M. H. P. Kole, Heteromeric Kv7.2/7.3 channels differentially regulate action potential initiation and conduction in neocortical myelinated axons. *J. Neurosci.* **34**, 3719–3732 (2014).
59. Y. Tay, J. Zhang, A. M. Thomson, B. Lim, I. Rigoutsos, MicroRNAs to Nanog, Oct4 and Sox2 coding regions modulate embryonic stem cell differentiation. *Nature* **455**, 1124–1128 (2008).
60. K. Zhang *et al.*, A novel class of microRNA-recognition elements that function only within open reading frames. *Nat. Struct. Mol. Biol.* **25**, 1019–1027 (2018).